Scouting Human A_3 Adenosine Receptor Antagonist Binding Mode Using a Molecular Simplification Approach: From Triazoloquinoxaline to a Pyrimidine Skeleton as a Key Study

Erika Morizzo,[†] Francesca Capelli,[‡] Ombretta Lenzi,[‡] Daniela Catarzi,[‡] Flavia Varano,[‡] Guido Filacchioni,[‡] Fabrizio Vincenzi,[§] Katia Varani,[§] Pier Andrea Borea,[§] Vittoria Colotta,*[,‡] and Stefano Moro*[,†]

Molecular Modeling Section, Dipartimento di Scienze Farmaceutiche, Università di Padova, via Marzolo 5, Padova, Italy, Dipartimento di Scienze Farmaceutiche, Laboratorio di Progettazione, Sintesi e Studio di Eterocicli Biologicamente Attivi, Università di Firenze, Polo Scientifico, Via Ugo Schiff, 6, 50019 Sesto Fiorentino, Italy, and Dipartimento di Medicina Clinica e Sperimentale, Sezione di Farmacologia, Università di Ferrara, via Fossato di Mortara 17-19, 44100 Ferrara

Received July 13, 2007

The concept of molecular simplification as a drug design strategy to shorten synthetic routes, while keeping or enhancing the biological activity of the lead drug, has been applied to design new classes of human A_3 adenosine receptor (AR) antagonists. Over the past decade, we have focused a part of our research on the study of AR antagonists belonging to strictly correlated classes of tricyclic compounds. One of these classes is represented by the 2-aryl-1,2,4-triazolo[4,3-*a*]quinoxalin-1-one derivatives, either 4-amino or 4-oxo-substituted, which were intensively investigated by evaluating the effect of different substituents on the 2-phenyl ring and on the 4-amino group. Using an in silico molecular simplification approach, a new series of easily synthesizable 2-amino/2-oxoquinazoline-4-carboxamido derivatives have been discovered, presenting high affinity and selectivity against human A_3 AR.

Introduction

The A_3 adenosine receptor (AR[a]) is one of the four G-protein-coupled receptors (GPCRs) activated by adenosine;[1] it is expressed in a broad spectrum of tissues and couples to $G_{i/o}$ proteins.[1,2] The ligand-stimulated A_3 AR leads to the elevation of intracellular Ca^{2+} concentration ($[Ca^{2+}]_i$) and the activation of phosphoinositide 3-kinase (PI3K)γ.[3,4] The activated PI3Kγ leads to the phosphorylation of protein kinase B (PKB) and members of the mitogen-activated protein kinase (MAPK) family, including extracellular signal-regulated kinase (ERK) 1/2 and p38.[3–5] This A_3 AR-stimulated PI3Kγ-dependent signaling pathway is essential for the potentiation of IgE/antigen-dependent mast cell degranulation[6] and the A_3 AR internalization.[7]

The A_3 AR is implicated in a variety of important physiological processes.[2] Activation of A_3 ARs increases the release of inflammatory mediators, such as histamine, from rodent mast cells[8] and inhibits the production of tumor necrosis factor-α.[9] The activation of the A_3 ARs is also suggested to be involved in immunosuppression and in the protection from ischemia of the brain and heart.[10] It is becoming increasingly apparent that agonists of A_3 ARs have potential as therapeutic agents for the treatment of rheumatoid arthritis and colorectal cancer, whereas antagonists might be therapeutically useful for the acute treatment of stroke and glaucoma and also as antiasthmatic and antiallergic drugs.[2,9,10]

Chart 1. Previously Reported 2-Aryl-1,2,4-triazolo[4,3-*a*]quinoxalin-1-ones (**TQX** Series)

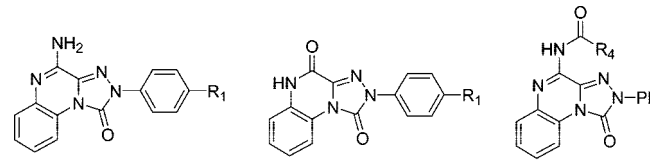

A R_1=H **C** R_1= OMe **B** R_1=H **D** R_1= OMe **E** R_4= Me **F** R_4= Ph

In particular, the development of antagonists for the A_3 ARs has so far been directed by traditional medicinal chemistry.[11] However, in the past few years we optimized a multidisciplinary integrated approach to speed up the discovery and the structural refinement of new potent and selective A_3 AR antagonists. Adenosine receptor antagonists, including A_3 AR-selective compounds, have been extensively reviewed in previous articles.[12–17]

Over the past decade, we have focused a part of our research on the study of AR antagonists belonging to strictly correlated classes of tricyclic compounds.[18–24] One of these classes is represented by the 2-aryl-1,2,4-triazolo[4,3-*a*]quinoxalin-1-one derivatives (**TQX** series), either 4-amino or 4-oxo-substituted, which were intensively investigated by evaluating the effect of different substituents on the 2-phenyl ring and on the 4-amino group (Chart 1).[18–21,24] These studies led to the identification of some groups which, introduced one by one in a suitable position of the parent compounds 4-amino-2-phenyl-1,2,4-triazolo[4,5-*a*]quinoxalin-1-one **A** and 2-phenyl-1,2,4-triazolo[4,5-*a*]quinoxalin-1,4-dione **B**, afforded high human (h) A_3 AR affinity and good selectivity.

These groups are the *para*-methoxy substituent on the 2-phenyl ring (compounds **C** and **D**)[18,24] and acyl residues, such as the acetyl or benzoyl groups, on the 4-amino group (compounds **E** and **F**).[18,24] However, besides potency and

* To whom correspondence should be addressed. Tel.: +39 049 8275704(S.M.); +39 55 4573731(V.C.). Fax: +39 049 827 5366 (S.M.); +39554573780(V.C.).E-mail: stefano.moro@unipd.it(S.M.); vittoria.colotta@unifi.it (V.C.).

[†] Università di Padova.

[‡] Università di Firenze.

[§] Università di Ferrara.

[a] Abbreviations: AR, adenosine receptor; h, human; TM, transmembrane; EL2, second extracellular loop; SAR, structure−affinity relationship; DPCPX, 8-cyclopentyl-1,3-dipropyl-xanthine; I-AB-MECA, N^6-(4-amino-3-iodobenzyl)-5′-(*N*-methylcarbamoyl)adenosine; NECA, 5′-(*N*-ethyl-carboxamido)adenosine; Cl-IB-MECA, 2-chloro-N^6-(3-iodobenzyl)-5′-(*N*-methylcarbamoyl)adenosine; GPCR, G-protein-coupled receptor; PI3Kγ, phosphoinositide 3-kinase γ; MAPK, mitogen-activated protein kinase; PKB, protein kinase B; ERK, extracellular signal-regulated kinase.

10.1021/jm070852a CCC: $37.00
Published on Web 11/30/2007

Chart 2. Hereby Reported 1,2,4-Triazoloquinoxalin-1-one Simplified Analogues

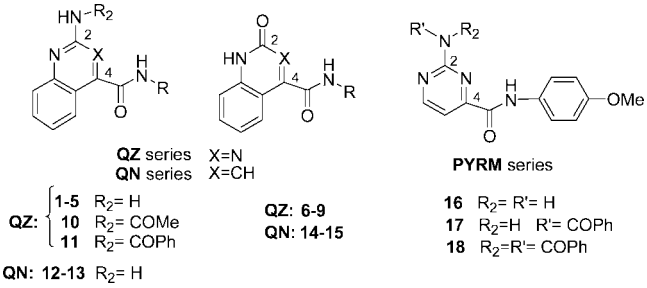

selectivity, the straightforward synthesis and pharmacokinetic profile represent crucial requirements in developing new possible therapeutic agents. Structural simplification represents a drug design strategy to shorten synthetic routes while keeping or enhancing the biological activity of the original candidate. Following this strategy, we have carried out an in silico molecular simplification approach to identify a suitable fragmentation route and explore which of the structural features are essential to guarantee an efficient ligand–receptor recognition. In this context, three series of triazoloquinoxalin-1-one analogues were prepared (Chart 2) and, among them, the easily synthesizable 2-amino/2-oxoquinazoline-4-carboxamido derivatives **1**–**11** (**QZ** series) proved to be highly potent and selective against the hA_3 AR.

Results and Discussion

In Silico Design of New 2-Aryl-1,2,4-triazolo[4,3-*a*]quinoxalin-1-one Simplified Analogues. As previously reported, 4-amino-2-aryl-1,2,4-triazolo[4,3-*a*]quinoxalin-1-one derivatives nicely bind to hA_3 AR.[18–24] We recognized the hypothetical binding site of the triazolo-quinoxalinone moiety surrounded by transmembrane (TM) regions 3, 5, 6, and 7, with the carbonyl group at the 1-position pointing toward the second extracellular loop (EL2) and the amide moiety in the 4-position oriented toward the intracellular environment.[21,24] The phenyl ring at the 2-position is positioned close to TM3, TM6, and TM7. The asymmetric topology of the binding cavity is characterized by a major axis (measured from TM1 toward TM5) of about 17 Å and by a minor axis (measured from TM3 toward TM6) of about 6 Å, as shown in Figure 1. The peculiar geometric properties of the hA_3 AR binding pocket effortlessly rationalize the experimental evidence that planar polyaromatic systems are usually suitable scaffolds to design potent and selective hA_3 AR antagonists. Moreover, planar polyaromatic systems seem to interact through $\pi-\pi$ stacking interactions at least with one of the two side chains of Phe168 (EL2) and Phe182 (5.43), as shown in Figure 1. This interaction has already been described as a crucial pharmacophoric feature in the hA_3 AR recognition.

All triazolo-quinoxalinone derivatives also share at least two stabilizing hydrogen-bonding interactions inside the binding cleft (Figure 1). The first hydrogen bonding is between the carbonyl group at the 1-position, which points toward the EL2, and the NH of the Gln167. This hydrogen-bonding distance is calculated around 2.7 Å for all docked compounds. Moreover, the 1-carbonyl group is also at the hydrogen-bonding distance with the amide moiety of Asn250 (6.55) side chain. This asparagine residue, conserved among all adenosine receptor subtypes, was found to be important for ligand binding. Second, the NH_2 or NHR moiety at the 4-position is surrounded by three polar amino acids: Thr94 (3.36), His95 (3.37), and Ser247 (6.52). This region seems to be very critical for the recognition of all antagonist structures. In fact, a major structural difference between the hypothetical binding sites in these receptor subtypes is that the hA_3 receptor does not contain the histidine residue in TM6 (6.52), common to all A_1 (His251 in hA_1) and A_2 (His250 in hA_{2A} and His251 in hA_{2B}) receptors. This histidine has been shown to participate in both agonist and antagonist binding to A_{2A} receptors. In the A_3 receptor, this histidine in TM6 is replaced by a serine residue (Ser247 in hA_3).[1,2]

Starting from these binding requirements, we decided to perform an in silico molecular simplification approach to identify a suitable fragmentation route of the 4-amino-triazoloquinoxalin-1-one scaffold and explore which of the structural features were essential to guarantee an efficient ligand–receptor recognition. A schematic representation of our molecular simplification is shown in Figure 2.

The first step was to verify the effects of the 4-amino-triazoloquinoxalin-1-one (**TQX** series) replacement with the 2-amino-quinazoline scaffold bearing a CO-NH-C_6H_4-R_1 moiety at the 4-position (**QZ** series). Interestingly, the formation of an intramolecular H-bond between the nitrogen at the 3-position of the quinazoline system and the NH of the amide moiety at the 4-position simulates the presence of a planar tricycle with similar steric properties with respect to the original triazoloquinoxalinone analog. Quantum chemistry calculations support the crucial role of the intramolecular H-bond in stabilizing the cyclic conformer (see Supporting Information for more details). Indeed, it is worth noting that a different entropy contribution, between the **TQX** and the **QZ** series, could differently affect the total free energy of binding. Unfortunately, in our docking simulations, the entropy effect could not accurately be taken into account. In particular, using the 4-amino-2-(4-methoxyphenyl)-triazoloquinoxalin-1-one derivative **C** (Chart 1) as primary reference compound, the corresponding 2-aminoquinazoline-4-carboxyamide derivative **1** (Chart 2, R = C_6H_4-*p*-OMe) was investigated. As shown in Figure 3, molecular docking simulations confirm that the new compound **1** is efficiently accommodated in the TM binding cavity, maintaining all crucial interactions above-mentioned ($\pi-\pi$ stacking interactions at least with both side chains of Phe168 (EL2) and Phe182 (5.43), two H-bonds with Gln167 (EL2) and Asn250 (6.55), and a H-bond interaction with His95 (3.37). In particular, His95 (3.37) is involved in a H-bond interaction with the amino group at the 2-position of the quinazoline-4-carboxyamide moiety. Analogously, we decided to extend our investigation, also considering the corresponding 2-oxo analogue of **1**, that is, the 2-oxo-quinazoline-4-carboxyamide derivative **6** (Chart 2, R = C_6H_4-*p*-OMe), which can also be considered the simplified analogue of the triazoloquinoxalin-1,4-dione derivative **D** (Chart 1). As is clearly shown in Figure 3, the 2-oxo derivative **6** assumes a binding conformation very similar to that of the 2-amino-quinazoline derivative **1**. In compound **6**, the 2-oxo group interacts through a H-bond interaction with His95 (3.37).

Subsequently, docking studies were also carried out to evaluate whether the presence of acyl residues on the 2-amino group of the new quinazoline-4-carboxamido series (Figure 2, **QZ** series, R_2 = acyl) was tolerated. The docking simulations, performed on the 2-acetylaminoquinazoline-4-carboxyanilide **10** (Chart 2, R = Ph) showed that the acetyl substituent is not only well tolerated, but it might reinforce the binding to the hA_3 AR (Figure 3). Indeed, consistently with that observed in the triazoloquinoxaline series,[24] an additional H-bond interaction takes place between the carbonyl moiety of the 2-acylamino group and the side chain of Ser247 (6.52).

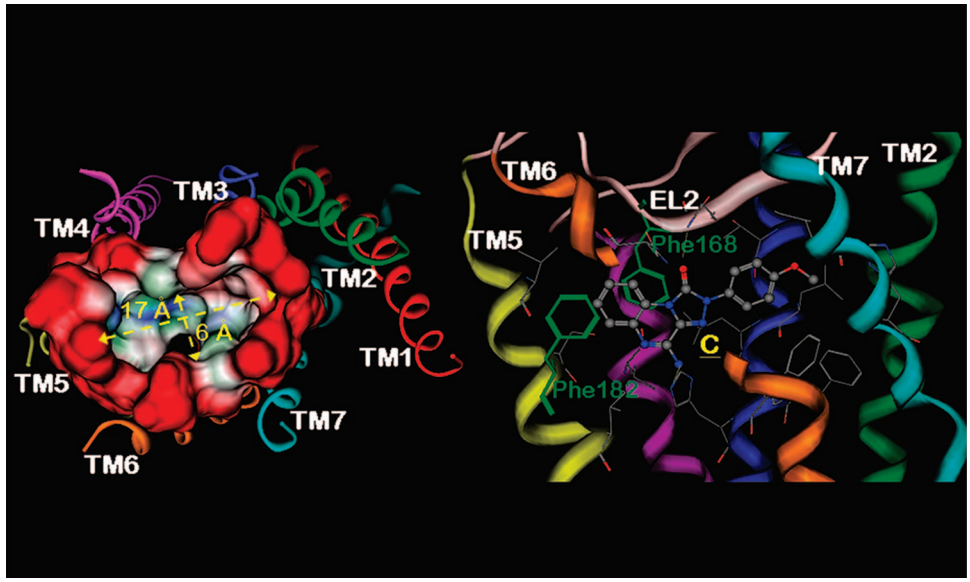

Figure 1. Hypothetical TM binding cleft topology of the human A_3 receptor model obtained by the conventional rhodopsin-based homology modeling approach (on the left); and hypothetical binding motif of the reference derivative **C** (on the right). The most energetically favorable docked conformation is viewed from the membrane side facing TM helices 5, 6, and 7. To clarify the TM cavity, the view of TM6 from Pro245 to Cys251, was voluntarily omitted. Side chains of some amino acids, important for ligand recognition, are highlighted. Hydrogen atoms are not displayed.

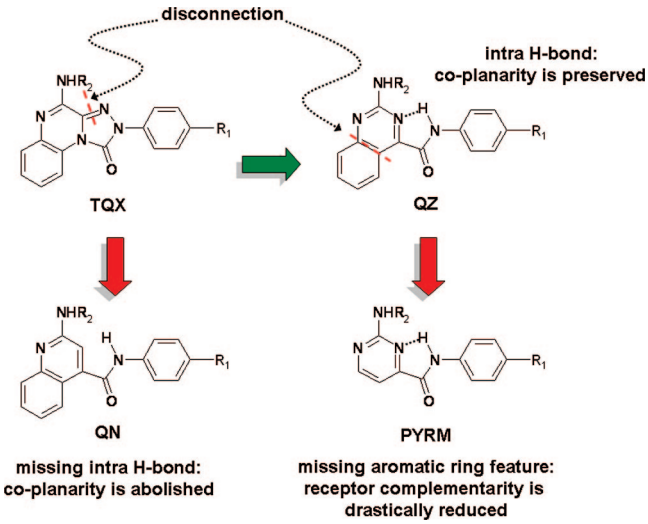

Figure 2. Flowchart of our in silico simplification approach.

To demonstrate the important role of the intramolecular H-bond interaction in maintaining the coplanarity of both 2-amino- and 2-oxo-quinazoline scaffolds and the CO-NHC_6H_4-R_1 moiety at the 4-position, we decided to design a new class of analogs: the 2-aminoquinoline-4-carboxamides (Figure 2, **QN** series) and the corresponding 2-oxo derivatives. In fact, in these quinoline derivatives, the formation of the intramolecular H-bond is not allowed and, consequently, the CO-NHC_6H_4-R_1 is twisted with respect to the quinoline ring of about 135°, as suggested by the systematic conformational analysis of the corresponding dihedral angle (data not shown). The impossibility of both 2-amino- and 2-oxo-quinoline systems to adopt a planar conformation is also confirmed by the docking simulations. In fact, as shown in Figure 4 for the 2-aminoquinoline-4-carboxyamide derivative **12** (Chart 2, R = C_6H_4-*p*-OMe) and its 2-oxo analogue **14** (Chart 2, R = C_6H_4-*p*-OMe), the corresponding energetically more stable docking pose is still twisted (of about 121°) and, in this conformation, the 2-amino-quinoline derivatives completely missed some of the most important interactions (in particular, the two H-bonds with Gln167 and Asn250) and drastically reduced their cavity shape complementarity.

Finally, to explore how reducible was the extension of the planar aromatic ring, starting from a 2-aminoquinazoline scaffold, we designed the corresponding 2-aminopyrimidines bearing a CO-NHC_6H_4-R_1 moiety at the 4-position (Figure 2, **PYRM** series). As above-described for the quinazoline derivatives, also in this series, we can observe the formation of the intramolecular H-bond between the 3-nitrogen atom of the pyrimidine system and the NH of the 4-amide moiety, which allows a simulation of the presence of a planar bicycle with a missing benzene ring, with respect to the original triazolo-quinoxalinone analogs. As shown in Figure 5 for the 2-aminopyrimidine-4-carboxy-(4-methoxyphenyl)amide **16** (Chart 2), molecular docking simulations indicate that 2-amino-pyrimidine skeleton maintains the stabilizing $\pi-\pi$ stacking interactions with both Phe168 and Phe182. However, the shift of the ligand position into the binding cleft abolishes the possibility an interaction through the H-bond with His95, Gln167, and Asn250, reducing the stability of the corresponding antagonist/receptor complex.

From these theoretical hypotheses, we synthesized and pharmacologically characterized some derivatives belonging to the three designed classes of triazolo-quinoxalinone simplified analogs (see Chart 2, Tables 1 and 2), that is, the 2-amino/2-oxoquinazoline-4-carboxamides **1**–**11** (**QZ** series), the 2-amino/2-oxoquinoline-4-carboxamides **12**–**15** (**QN** series), and the 2-aminopyrimidine-4-carboxyamides **16**–**18** (**PYRM** series). Among these compounds, there are the above cited and theoretically investigated quinazolines **1**, **6**, and **10**, quinolines **12** and **14**, and pyrimidines **16**, all except one (**10**) bearing the 4-carboxy-(4-methoxyphenyl)amide function. To perform a preliminary structure−affinity relationship (SAR) study, in the first two series, we synthesized derivatives lacking the methoxy group on the 4-carboxyamide moiety, that is, the 4-carboxyanilide compounds **2**, **7**, **13**, and **15**. In the quinazoline series, the methoxy group was also replaced by lipophilic substituents, such as methyl (compounds **3** and **8**) or bromine (compounds **4** and **9**). In addition, to evaluate the importance of the aromatic

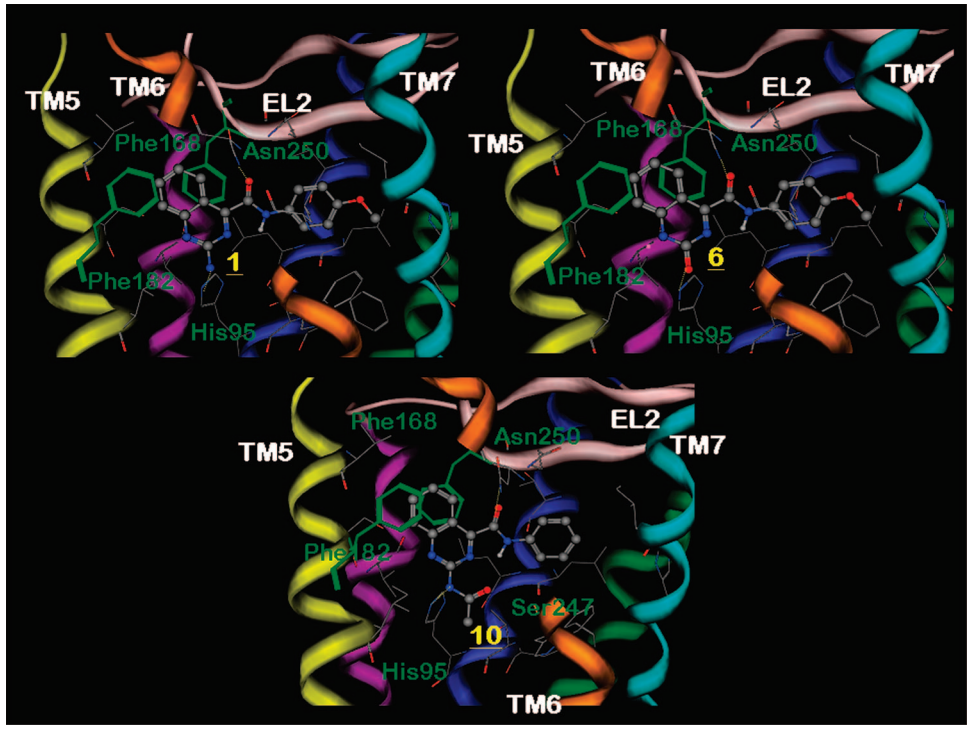

Figure 3. Hypothetical binding motif of the newly synthesized A_3 antagonists: **1** (top on the left), **6** (top on the right), and **10** (bottom). The most energetically favorable docked conformations are viewed from the membrane side facing TM helices 5, 6, and 7. To clarify the TM cavity, the view of TM6 from Pro245 to Cys251 was voluntarily omitted. Side chains of some amino acids, important for ligand recognition, are highlighted. Hydrogen atoms are not displayed.

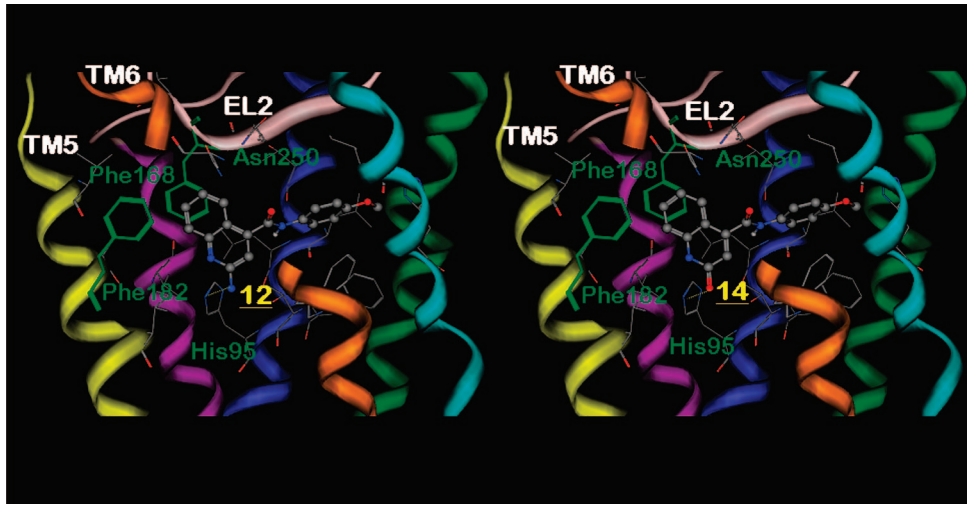

Figure 4. Hypothetical binding motif of the newly synthesized analogs **12** (on the left) and **14** (on the right). The most energetically favorable docked conformations are viewed from the membrane side facing TM helices 5, 6, and 7. To clarify the TM cavity, the view of TM6 from Pro245 to Cys251 was voluntarily omitted. Side chains of some amino acids important for ligand recognition are highlighted. Hydrogen atoms are not displayed.

phenyl ring on the carboxyamide function, the 2-aminoquinazoline-4-carboxy-cyclohexylamide **5** was synthesized. The effect of a benzoyl residue on the 2-amino function was evaluated both in the quinazoline (compound **11**) and in the pyrimidine (compound **17**) series, and in the latter, the 2-dibenzoylamino derivative **18** was also prepared.

Chemistry

The quinazoline-4-carboxamido derivatives **1**–**11**, their 3-deaza analogues quinoline-4-carboxamides **12**–**15**, and the pyrimidine-4-carboxamides **16**–**18** were obtained as depicted in Schemes 1 and 2. Scheme 1 showed the straightforward synthesis of the 2-amino-quinazoline-4-carboxamido derivatives **1**–**5** and the 2-oxo-quinazoline-4-carboxamido derivatives **6**–**9**, which were prepared by coupling the corresponding 2-amino- and 2-oxo-quinazoline-4-carboxylic acids[25] with the suitable amines **19**–**23** (Scheme 1). By reaction of the 2-amino-quinazoline-4-carboxyanilide **2** with acetyl and benzoyl chloride, the 2-amido-quinazoline-4-carboxyamides **10** and **11** were obtained, respectively. The 2-aminoquinoline-4-carboxamides **12** and **13** (Scheme 2) were synthesized starting from the 2-chloroquinoline-4-carboxamides **24** and **25**,[26,27] which were reacted with hydrazine monohydrate under microwave irradiation to yield the corresponding 2-hydrazinoquinoline-4-car-

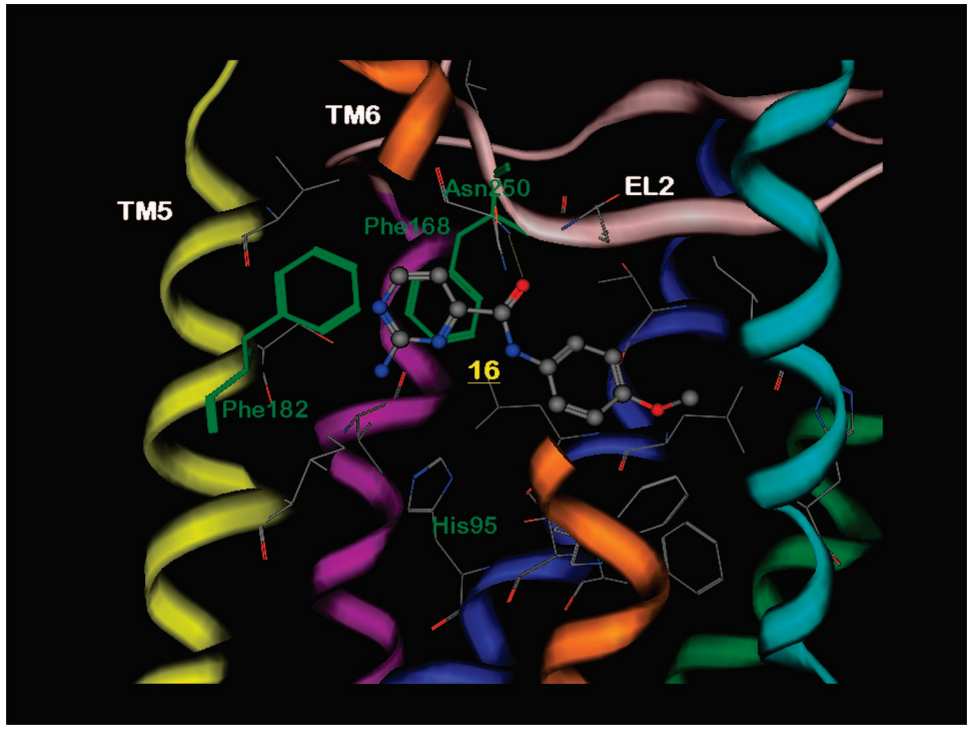

Figure 5. Hypothetical binding motif of the newly synthesized analog **16**. The most energetically favorable docked conformation is viewed from the membrane side facing TM helices 5, 6, and 7. To clarify the TM cavity, the view of TM6 from Pro245 to Cys251 was voluntarily omitted. Side chains of some amino acids important for ligand recognition are highlighted. Hydrogen atoms are not displayed.

Scheme 1[a]

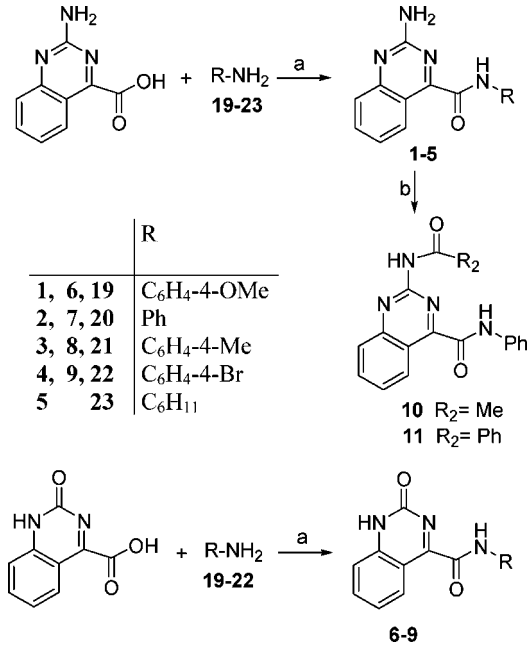

[a] Reagents: (a) R-NH_2, 1-hydroxybenzotriazole, NEt_3, 4-(dimethylamino)pyridine, 1-(3-(dimethylamino)propyl)-3-ethylcarbodiimide hydrochloride, DMF; (b) R-COCl, anhydrous pyridine, methylene chloride.

Scheme 2[a]

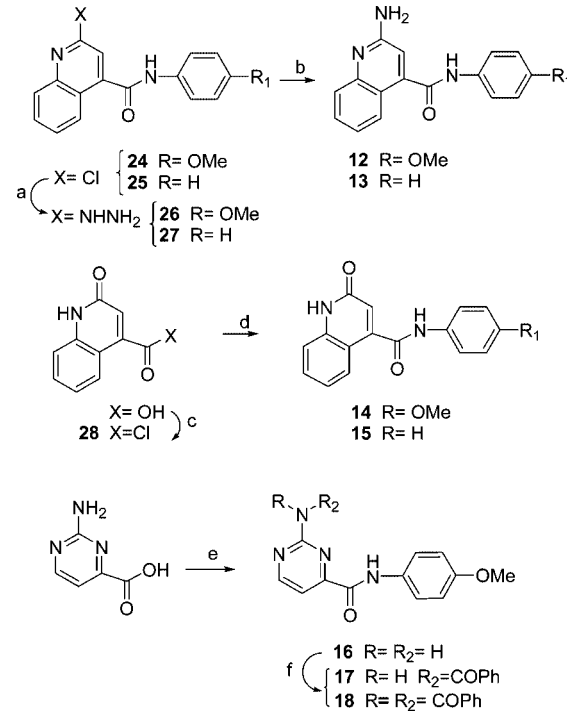

[a] Reagents: (a) hydrazine monohydrate, EtOH, microwave irradiation; (b) H_2, Ni/Raney, EtOH; (c) thionyl chloride; (d) aniline derivative, Et_3N, anhydrous methylene chloride; (e) 4-methoxyaniline, 1-hydroxybenzotriazole, NEt_3, 4-(dimethylamino)pyridine, 1-(3-(dimethylamino)propyl)-3-ethylcarbodiimide hydrochloride, DMF; (f) PhCOCl, anhydrous pyridine, methylene chloride.

boxyamides **26** and **27**.[26,27] Hydrazinolysis of compounds **26** and **27** afforded the desired 2-aminoquinoline derivatives **12** and **13**. Synthesis of 2-oxo-1,2-dihydroquinoline-4-carboxamides **14** and **15** was achieved by reacting suitable aniline derivatives with the 2-oxo-1,2-dihydroquinoline-4-carbonyl chloride **28**, obtained from the corresponding 2-oxo-1,2-dihydroquinoline-4-carboxylic acid[28] in boiling thionyl chloride. The 2-aminopyrimidine-4-carboxamido compounds **16**–**18** were prepared starting from the 2-aminopyrimidine-4-carboxylic acid,[29] which was reacted with 4-methoxyaniline to give the 2-aminopyrimidine-4-carboxamide **16**. Reaction of **16** with benzoyl chloride gave a mixture of the 2-benzoylamino- and 2-dibenzoylamino-

Table 1. Binding Affinity (K_i) at hA_1, hA_{2A}, and hA_3 ARs and Potency (IC_{50}) at hA_{2B} and A_3 ARs

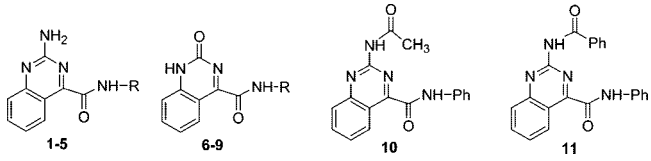

		K_i (nM) or *I*%			IC$_{50}$ (nM) or *I*% cAMP	
	R	hA_3[a]	hA_1[b]	hA_{2A}[c]	hA_{2B}[d]	hA_3[e]
1	C_6H_4-4-OMe	87.5 ± 6.6	8%	6%	23%	
2	C_6H_5	350 ± 40	40%	17%	5%	
3	C_6H_4-4-Me	98.3 ± 7.3	3%	5%	4%	
4	C_6H_4-4-Br	550 ± 47	1%	1%	2%	
5	C_6H_{11}	21%	2%	3%	1%	
6	C_6H_4-4-OMe	19.5 ± 2.2	4%	1%	9%	125 ± 10
7	C_6H_5	50 ± 4	22%	1%	4%	238 ± 21
8	C_6H_4-4-Me	26.7 ± 3.3	21%	2%	2%	
9	C_6H_4-4-Br	27.2 ± 3.1	3%	1%	2%	
10		25.3 ± 2.8	25%	7%	5%	140 ± 13
11		182 ± 10	7%	10%	3%	

[a] Displacement of specific [^{125}I]AB-MECA binding to hA_3 CHO cells. K_i values are means ± SEM of four separate assays, each performed in duplicate. [b] Percentage of inhibition in [^{3}H]DPCPX competition binding assays to hA_1 CHO cells at 1 μM concentration of the tested compounds. [c] Percentage of inhibition in [^{3}H]ZM241385 competition binding assays to hA_{2A} CHO cells at 1 μM concentration of the tested compounds. [d] Percentage of inhibition on cAMP experiments in hA_{2B} CHO cells, stimulated by 200 nM NECA, at 1 μM concentration of the examined compounds. [e] IC_{50} values are expressed as means ± SEM of four separate cAMP experiments in hA_3 CHO cells, inhibited by 100 nM Cl-IB-MECA.

derivatives **17** and **18**, which were separated by column chromatography.

Pharmacological Assays

All the synthesized derivatives **1–18** were tested to evaluate their affinity at hA_1, hA_{2A}, and hA_3 ARs. Compounds **1–18** were also tested at the hA_{2B} subtype by measuring their inhibitory effects on NECA-stimulated cAMP levels in CHO cells stably transfected with the hA_{2B} AR. Finally, the antagonistic potencies of the three selected quinazoline derivatives **6**, **7**, and **10** were assessed by evaluating their inhibition on Cl-IB-MECA-inhibited cAMP production in CHO cells, stably expressing hA_3 ARs. All pharmacological data are collected in Tables 1 and 2.

SAR Commentary. Impressively, the pharmacological data, reported in Tables 12, are coherent with the predictions based on our in silico simplification approach. In fact, the new quinazoline derivatives **1–11** are potent antagonists at the hA_3 AR and are also highly selective, being completely inactive at the other AR subtypes (Table 1). The antagonist properties at the hA_3 AR of this series of simplified triazoloquinoxalinone analogues were assessed by testing three selected derivatives (**6**, **7**, and **10**) in the AMPc assays. Compounds **6**, **7**, and **10** antagonized the Cl-IB-MECA-inhibited cAMP production with potencies in accordance with the hA_3 AR affinities.

In contrast to the high hA_3 AR affinity of the quinazoline derivatives **1–11**, but consistent with the predictions, the quinoline derivatives **12–15**, as well as the pyrimidine compounds **16–18**, completely lacked affinities at the hA_3 AR (Table 2). In fact, at 1 μM concentration, they inhibited the radioligand binding at this subtype, as well as at hA_1 and hA_{2A} ARs, for only 1–38%. Compounds **12–18** were also inactive in inhibiting the NECA-stimulated cAMP accumulation in hA_{2B} CHO cells (*I*% = 2–5%).

The structure−affinity relationships (SAR) in the quinazoline series resemble those previously observed in the leads.[18,24] It is confirmed that the advantageous role of the *p*-methoxy substituent, indeed its removing from the 4-carboxamide phenyl ring, which mimics the 2-phenyl ring of the triazoloquinoxaline derivatives, caused a reduction of the hA_3 AR affinity (compare the 4-carboxy-(p-methoxyphenyl)amides **1** and **6** with the corresponding 4-carboxyanilides **2** and **7**). Replacement of the *para*-methoxy residue (compounds **1** and **6**) with lipophilic substituents, such as the methyl (derivatives **3** and **8**) or bromine (compounds **4** and **9**), maintained the hA_3 affinity in the nanomolar range, the only exception being compound **4**, which possesses a 5-fold reduced binding activity, compared to derivative **1**. The profitable effect of the above cited groups is coherent with the observation that these residues are positioned in a small hydrophobic pocket in between TM3 and TM7.

As observed in the triazoloquinoxalin-1-one series,[18,24] replacement of the 2-amino group with the 2-oxo residue is advantageous for the anchoring to the A_3 AR binding site (compare **6–9** with **1–4**), in particular, due to a probably stronger H-bond interaction with His95 (3.37).

In agreement with our previous findings in the triazoloquinoxalin-1-one derivatives[18,24] and with the docking predictions, introduction of acyl substituents on the 2-amino group enhances the hA_3 AR affinity (compare compounds **10** and **11** with

Table 2. Inhibition of Specific Binding at hA_1, hA_{2A}, and hA_3 ARs and of cAMP Production at hA_{2B} AR

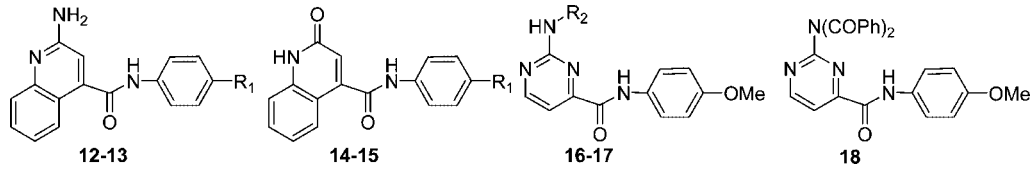

			binding experiments			cAMP assays
	R_1	R_2	hA_3[a]	hA_1[b]	hA_{2A}[c]	hA_{2B}[d]
13	H		6%	1%	2%	5%
12	OMe		1%	2%	3%	3%
14	OMe		26%	4%	1%	3%
15	H		38%	1%	1%	2%
16		H	15%	3%	6%	3%
17		COPh	22%	6%	6%	2%
18			14%	5%	1%	3%

[a] Percentage of inhibition in [^{125}I]AB-MECA competition binding assays to hA_3CHO cells at 1 μM concentration of the tested compounds. [b] Percentage of inhibition in [^{3}H]-DPCPX competition binding assays to hA_1CHO cells at 1 μM concentration of the tested compounds. [c] Percentage of inhibition in [^{3}H]-ZM 241385 competition binding assays to hA_{2A}CHO cells at 1 μM concentration of the tested compounds. [d] Percentage of inhibition on cAMP experiments in hA_{2B} CHO cells, stimulated by 200 nM NECA, at 1 μM concentration of the tested compounds.

Table 3. Comparison between the hA_3 AR Affinities of the Quinazoline-4-carboxamides and the Corresponding Triazoloquinoxalin-1-ones

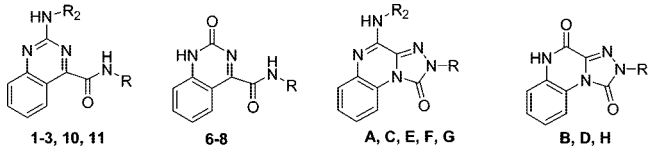

		K_i (nM) hA_3			
		quinazolines[a]		triazoloquinoxalines[b]	
R	R_2				
C_6H_4-*p*-OMe	H	**1**	87.5 ± 6.6	**C**	45.3 ± 3.8
C_6H_5	H	**2**	350 ± 40	**A**	490 ± 41
C_6H_4-*p*-Me	H	**3**	98.3 ± 7.3	**G**	48.3 ± 3.6
C_6H_4-*p*-OMe		**6**	19.5 ± 2.2	**D**	16 ± 1.2
C_6H_5		**7**	50 ± 4	**B**	80 ± 4
C_6H_4-*p*-Me		**8**	26.7 ± 3.3	**H**	25.0 ± 1.6
C_6H_5	COMe	**10**	25.3 ± 2.8	**E**	2.0 ± 0.13
C_6H_5	COPh	**11**	182 ± 10	**F**	1.47 ± 0.1

[a] Data from Table 1. [b] Data from refs 18, 19, and 21.

derivative **2**), probably because of the hydrogen-bonding interaction that the acyl oxygen engages with the Ser247 side chain.

Replacement of the 4-carboxyanilide moiety of compound **2** with a 4-carboxycyclohexylamide group (compound **5**) dramatically affected the hA_3 affinity. As already described, the asymmetric topology of the TM binding cavity, characterized by a major axis of about 17 Å and by a minor axis of about 6 Å, does not allow to accommodate the bulky cyclohexyl moiety, causing an unfavorable van der Waals repulsive interaction (data not shown).

Finally, it has to be pointed out that, on the whole, the hA_3 AR affinities of the quinazoline-4-carboxamido derivatives are comparable to those of the corresponding triazoloquinoxalin-1-one leads,[18,19,21] as it appears by comparing the hA_3 AR binding data of some derivatives of the two series (Table 3). There are two exceptions: the 2-acylamino derivatives **10** and **11** that possess, respectively, a 10- and 120-fold reduced affinity, in comparison to that of corresponding parent compounds **E** and **F**. Moreover, another relevant finding was the higher solubility of the new quinazoline derivatives. Indeed, experimentally, the quinazolines derivatives showed a significantly enhanced solubility in the most common organic solvents with respect to that of the tryciclic parent derivatives.

Conclusions

As already reported, rhodopsin-based homology modeling represents a widely used and well-consolidated approach to visualize GPCR three-dimensional models. Modeling ligand–receptor complexes, as provided by the crystallographic structure of rhodopsin, enables the study of specific interactions at higher resolution. In this paper we have once again demonstrated, by using our in silico simplification approach, how crucial computational models are to generate hypotheses and how the experimental findings are, in turn, used to refine the model. The success of this approach is due to the synergistic interaction between theory and experiment. Indeed, within the new easily synthesizable quinazoline-4-carboxyamide series, we have identified some highly potent and selective hA_3 AR antagonists and we have clarified which chemical features are crucial to efficiently recognize the TM binding cleft.

Experimental Section

(A) Computational Methodologies. All modeling studies were carried out on a 10 CPU (PIV-3.0GHZ and AMD64) linux cluster.

Homology modeling, energy calculation, and docking studies were performed using the Molecular Operating Environment (MOE, version 2006.08) suite.[37]

All docked structures were fully optimized without geometry constraints using RHF/AM1 semiempirical calculations. Vibrational frequency analysis was used to characterize the minima stationary points (zero imaginary frequencies). The software package MOPAC (ver. 7),[38] implemented in MOE suite, was utilized for all quantum mechanical calculations.

Homology Model of the hA_3 AR. Based on the assumption that GPCRs share similar TM boundaries and overall topology, a homology model of the hA_3 receptor was constructed. First, the amino acid sequences of TM helices of the A_3 receptor were aligned with those of bovine rhodopsin, guided by the highly conserved amino acid residues, including the DRY motif (D3.49, R3.50, and Y3.51) and three proline residues (P4.60, P6.50, and P7.50) in the TM segments of GPCRs. The same boundaries were applied for the TM helices of the A_3 receptor as they were identified from the X-ray crystal structure for the corresponding sequences of bovine rhodopsin,[39] the C_R coordinates of which were used to construct the seven TM helices for the hA_3 receptor. The loop domains of the hA_3 receptor were constructed by the loop search method implemented in MOE. In particular, loops are modeled first in random order. For each loop, a contact energy function analyzes the list of candidates collected in the segment searching stage, taking into account all atoms already modeled and any atoms specified by the user as belonging to the model environment. These energies are then used to make a Boltzmann-weighted choice from the candidates, the coordinates of which are then copied to the model. Any missing side chain atoms are modeled using the same procedure. Side chains belonging to residues whose backbone coordinates were copied from a template are modeled first, followed by side chains of modeled loops. Outgaps and their side chains are modeled last. Special caution has to be given to the EL2, which has been described in bovine rhodopsin as folding back over transmembrane helices and, therefore, limiting the size of the active site.[39] Hence, amino acids of this loop could be involved in direct interactions with the ligands. A driving force to this peculiar fold of the EL2 loop might be the presence of a disulfide bridge between cysteines in TM3 and EL2. Because this covalent link is conserved in all receptors modeled in the current study, the EL2 loop was modeled using a rhodopsin-like constrained geometry around the EL2-TM3 disulfide bridge. After the heavy atoms were modeled, all hydrogen atoms were added, and the protein coordinates were then minimized with MOE using the AMBER94 force field.[40] The minimizations were carried out by the 1000 steps of steepest descent followed by conjugate gradient minimization until the rms gradient of the potential energy was less than 0.1 kcal mol^{-1} $Å^{-1}$. Protein stereochemistry evaluation was performed by several tools (Ramachandran and Chi plots measure phi/psi and chi1/chi2 angles, clash contacts reports) implemented in the MOE suite.[37]

Considering the acceptable topological complementarity of all A_3 antagonists described in the present work, our recently proposed ligand-based homology modeling approach has been not carried out.[41]

Molecular Docking of the hA_3 AR Antagonists. All antagonist structures were docked into the hypothetical TM binding site by using the MOE-dock tool, part of the MOE suite. Searching is conducted within a user-specified 3D docking box (the standard protocol selects all atoms inside 12 Å from the center of mass of the binding cavity), using the Tabu Search[42] protocol (standard parameters are: 1000 steps/run, 10 attempts/step, and 10 Tabu list length), and the MMFF94 force field.[43] MOE-dock performs a user-specified number of independent docking runs (50 in our specific case) and writes the resulting conformations and their energies in a molecular database file. The resulting docked complexes were subjected to MMFF94 energy minimization until the rms of

Table 4. Predicted Binding Affinity (pK_i) of the Most Relevant New Simplified Triazoloquinoxaline Analogs

#	pK_i[a]
C	6.6
1	6.6
6	7.3
10	7.2
12	4.8
14	5.1
16	4.6

[a] pK_i values were calculated and visualized using the MOE-scoring tool implemented into the MOE suite.[37]

conjugate gradient was <0.1 kcal mol^{-1} Å^{-1}. Charges for the ligands were imported from the MOPAC output files. To better refine all antagonist−receptor complexes, a rotamer exploration of all side chains involved in the antagonist-binding was carried out. Rotamer exploration methodology was implemented in the MOE suite.[37] Prediction of antagonist−receptor complex stability (in terms of corresponding pK_i value) and the quantitative analysis for nonbonded intermolecular interactions (H-bonds, transition metal, water bridges, hydrophobic) were calculated and visualized using the MOE-scoring tool implemented into the MOE suite.[37] A summary of the most relevant pK_i value predictions are collected in Table 4.

(B) Chemistry. The microwave-assisted syntheses were performed using an Initiator EXP Microwave Biotage instrument (frequency of irradiation: 2.45 GHz). Silica gel plates (Merck F_{254}) and silica gel 60 (Merck, 70–230 mesh) were used for analytical and column chromatography, respectively. All melting points were determined on a Gallenkamp melting point apparatus. Microanalyses were performed with a Perkin-Elmer 260 elemental analyzer for C, H, N, and the results were within ±0.4% of the theoretical values, unless otherwise stated. The IR spectra were recorded with a Perkin-Elmer Spectrum RX I spectrometer in Nujol mulls and are expressed in cm^{-1}. The ^{1}H NMR spectra were obtained with a Brucker Avance 400 MHz instrument. The chemical shifts are reported in δ (ppm) and are relative to the central peak of the solvent, which was always DMSO-d_6. The following abbreviations are used: s = singlet, d = doublet, t = triplet, m = multiplet, br = broad, and ar = aromatic protons.

General Procedure for the Synthesis of 2-Aminoquinazoline-4-carboxamido Derivatives 1–5. An excess of 2-aminoquinazoline-4-carboxylic acid[25] (2.64 mmol) was reacted with the amines **19**, **21**–**23** (0.88 mmol), and **20** (1.32 mmol), in the presence of 1-(3-(dimethylamino)propyl))-3-ethyl-carbodiimide hydrochloride (2.64 mmol), 1-hydroxybenzotriazole (2.64 mmol), triethylamine (4.4 mmol), and 4-(dimethylamino)pyridine (0.08 mmol) in anhydrous dimethylformamide (2–3 mL). The mixture was stirred at room temperature for 26 h (compound **3**), 96 h (compounds **1**, **4**, and **5**), and 168 h (compound **2**). The title compounds were obtained by a different workup of the reaction mixtures.

2-Aminoquinazoline-4-carboxy-(4-methoxyphenyl)amide (1). The insoluble solid was filtered off from the reaction mixture and water was added to the cooled (0 °C) dimethylformamide solution until a solid was obtained, which was collected and recrystallized. Yield, 63%; mp 217–220 °C (EtOH); ^{1}H NMR 3.77 (s, 3H, OMe), 6.97 (d, 2H, ar, J = 8.3 Hz), 7.08 (s, 2H, NH_2), 7.26 (t, 1H, ar, J = 7.3 Hz), 7.51 (d, 1H, ar, J = 8.2 Hz), 7.70–7.76 (m, 3H, ar), 8.10 (d, 1H, ar, J = 8.4 Hz), 10.66 (s, 1H, NH); IR 1664, 3303, 3437; Anal. ($C_{16}H_{14}N_4O_2$) C, H, N.

2-Aminoquinazoline-4-carboxyanilide (2). The insolubile solid was collected by filtration and washed with water. A second crop of solid was obtained by dilution with water of the cooled (0 °C) mother liquor. The two solids were put together and recrystallized. Yield, 54%; mp 191–193 °C (EtOH); ^{1}H NMR 7.12 (s, 2H, NH_2), 7.17 (t, 1H, ar, J = 7.4 Hz), 7.27 (t, 1H, ar, J = 7.6 Hz), 7.41 (t, 2H, ar, J = 7.8 Hz), 7.52 (d, 1H, ar, J = 8.4 Hz), 7.73–7.80 (m, 3H, ar), 8.07 (d, 1H, ar, J = 8.4 Hz), 10.82 (s, 1H, NH); IR 1664, 3303, 3462; Anal. ($C_{15}H_{12}N_4O$) C, H, N.

2-Aminoquinazoline-4-carboxy-(4-methylphenyl)amide (3), 2-Aminoquinazoline-4-carboxy-(4-bromophenyl)amide (4). The title compounds were obtained from the reaction mixture, as described above for compound **1**. **Compound 3:** yield, 78%; mp 293–295 °C (EtOH); ^{1}H NMR 2.30 (s, 3H, Me), 7.11 (s, 2H, NH_2), 7.19–7.26 (m, 3H, ar), 7.51 (d, 1H, ar, J = 8.4 Hz), 7.66–7.74 (m, 3H, ar), 8.06 (d, 1H, ar, J = 8.1 Hz), 10.74 (s, 1H, NH); IR 1664, 1688, 3321, 3385; Anal. ($C_{16}H_{14}N_4O$) C, H, N. **Compound 4:** yield, 76%; mp 244–247 °C (EtOH); ^{1}H NMR 7.11 (s, 2H, NH_2), 7.27 (t, 1H, ar, J = 7.9 Hz), 7.51–7.61 (m, 3H, ar), 7.73–7.76 (m, 3H, ar), 8.07 (d, 1H, ar, J = 8.3 Hz), 10.96 (s, 1H, NH); IR 1630, 1674, 3288, 3347, 3478; Anal. ($C_{15}H_{11}BrN_4O$) C, H, N.

2-Aminoquinazoline-4-carboxycyclohexylamide (5). The reaction mixture was a solution that was cooled at 0 °C and diluted with water (5–10 mL) to yield a solid, which was collected. Extraction of the mother liquor with chloroform (30 mL × 3) and evaporation of the anhydrified (Na_2SO_4) organic phases under reduced pressure gave a solid that, collected to the first, was recrystallized. Yield, 22%; mp 176–177 °C (EtOH); ^{1}H NMR 1.07–1.38 (m, 5H, cyclohexyl), 1.60−1.91 (m, 5H, cyclohexyl), 3.81–3.90 (m, 1H, cyclohexyl), 7.03 (s, 2H, NH_2), 7.24 (t, 1H, ar, J =7.6 Hz), 7.45 (d, 1H, ar, J = 8.4 Hz), 7.71 (t, 1H, ar, J = 7.6 Hz), 8.01 (d, 1H, ar, J = 8.32), 8.66 (d, 1H, NH, J = 7.7 Hz); IR 1637, 3297, 3464; Anal. ($C_{15}H_{18}N_4O$) C, H, N.

General Procedure for the Synthesis of 2-Oxoquinazoline-4-carboxamido Derivatives 6–9. An excess of 2-oxoquinazoline-4-carboxylic acid[25] (2.64 mmol) was reacted with the amines **19**, **21**, **22** (0.88 mmol), and **20** (0.59 mmol) in the presence of 1-(3-(dimethylamino)propyl))-3-ethyl-carbodiimide hydrochloride (2.64 mmol), 1-hydroxybenzotriazole (2.64 mmol), triethylamine (4.4 mmol), and 4-(dimethylamino)pyridine (0.08 mmol) in anhydrous dioxane (5 mL, derivative **7**) or anhydrous dimethylformamide (2–3 mL, compounds **6**, **8**, **9**). The mixture was stirred at room temperature for 4 h (compound **6**), 24 h (compound **8**), 72 h (compound **9**), or 168 h (compound **7**) The title compounds were obtained by different workup of the reaction mixtures.

1,2-Dihydro-2-oxoquinazoline-4-carboxy-(4-methoxyphenyl) amide (6). The solid was filtered off and the dimethylformamide was distilled at reduced pressure. By treating the residue with an EtOH/EtOAc mixture, a solid was obtained that was collected and recrystallized. Yield, 60%; mp > 300 °C (EtOH); ^{1}H NMR 3.77 (s, 3H, OMe), 6.97 (d, 2H, ar, J = 8.8 Hz), 7.29 (t, 1H, ar, J = 7.7 Hz), 7.38 (d, 1H, ar, J = 8.6 Hz), 7.71 (d, 2H, ar, J = 8.8 Hz), 7.79 (t, 1H, ar, J = 7.7 Hz), 8.07 (d, 1H, ar, J = 7.8 Hz), 10.79 (s, 1H, NH), 12.20 (s, 1H, NH); IR 1669, 3326; Anal. ($C_{16}H_{13}N_3O_3$) C, H, N.

1,2-Dihydro-2-oxoquinazoline-4-carboxyanilide (7). The solid was filtered off and the clear dioxane solution was diluted with water (15 mL) and extracted with chloroform (15 mL × 3). The organic phases were anhydrified, and the solvent was evaporated at reduced pressure to yield a solid, which was recrystallized. Yield, 48%; mp > 300 °C (2-ethoxyethanol); ^{1}H NMR 7.18 (t, 1H, ar, J = 7.3 Hz), 7.30 (t, 1H, ar, J = 7.7 Hz), 7.38–7.43 (m, 3H, ar), 7.78–7.83 (m, 3H, ar), 8.05 (d, 1H, ar, J = 8.2 Hz), 10.92 (s, 1H, NH), 12.02 (s, 1H, NH); IR 1666, 3319; Anal. ($C_{15}H_{112}N_3O_2$) C, H, N.

1,2-Dihydro-2-oxoquinazoline-4-carboxy-(4-methylphenyl)amide (8). The reaction mixture was diluted with water (15–20 mL) and extracted with chloroform (15 mL × 3). The anydrified (Na_2SO_4) organic phases were evaporated at reduced pressure to give an oil that solidified upon treatment with a few drops of EtOH and petroleum ether. Yield, 65%; mp 193–195 °C (EtOH); ^{1}H NMR 2.30 (s, 3H, Me), 7.21 (d, 2H, ar, J = 8.2 Hz), 7.29 (t, 1H, ar, J = 7.7 Hz), 7.38 (d, 1H, ar, J = 8.3 Hz), 7.67 (d, 2H, ar, J = 7.7 Hz), 7.80 (t, 1H, ar, J = 7.7 Hz), 8.02 (d, 1H, ar, J = 8.1 Hz), 10.82 (s, 1H, NH), 12.21 (s, 1H, NH); IR 1668, 3228; Anal. ($C_{16}H_{13}N_3O_2$) C, H, N.

1,2-Dihydro-2-oxoquinazoline-4-carboxy-(4-bromophenyl) amide (9). The cooled (0 °C) reaction mixture was diluted with water (15–20 mL), and the solid was collected by filtration and recrystallized. Yield, 67%; mp > 300 °C (EtOH); ^{1}H NMR 7.30

(t, 1H, ar, $J = 7.8$ Hz), 7.39 (d, 1H, ar, $J = 8.4$ Hz), 7.61 (d, 2H, ar, $J = 8.6$ Hz), 7.77–7.83 (m, 3H, ar), 8.07 (d, 1H, ar, $J = 8.1$ Hz), 11.08 (s, 1H, NH), 12.25 (s, 1H, NH); IR 1667, 3335; Anal. ($C_{15}H_{10}BrN_3O_2$) C, H, N.

Synthesis of 2-Acetylaminoquinazoline-4-carboxyanilide (10). Acetyl chloride (1.51 mmol) was added to a suspension of 2-aminoquinazoline derivative **2** (1.26 mmol) in anhydrous methylene chloride (20 mL) and pyridine (0.2 mL). The mixture was stirred at room temperature for 5 h. The solid was collected by filtration and washed with water. The methylene chloride solution was diluted with diethyl ether (10–15 mL) to yield a second crop of solid that was collected by filtration and, together with the first solid, recrystallized. Yield, 79%; mp 232–233 °C (EtOH); ^{1}H NMR 2.31 (s, 3H, Me), 7.19 (t, 1H, ar, $J = 7.3$ Hz), 7.42 (t, 2H, ar, $J = 7.4$ Hz), 7.61 (t, 1H, ar, $J = 7.1$ Hz), 7.81 (d, 2H, ar, $J = 7.4$ Hz), 7.91 (d 1H, ar, $J = 8.6$ Hz), 8.01 (t, 1H, ar, $J = 8.5$ Hz), 8.41 (d, 1H, ar, $J = 8.5$ Hz), 10.92 (s, 2H, 2NH); IR 1680, 3322; Anal. ($C_{17}H_{14}N_4O_2$) C, H, N.

Synthesis of 2-Benzoylaminoquinazoline-4-carboxyanilide (11). Benzoyl chloride (1.26 mmol) was added to a suspension of 2-aminoquinazoline derivative **2** (1.26 mmol) in anhydrous methylene chloride (20 mL) and pyridine (0.2 mL). The reaction mixture was refluxed for 30 h, and after cooling, the solid was collected by filtration and washed with water. The clear solution was evaporated under reduced pressure to afford a solid that, collected with the first solid, was chromatographed on a silica gel column (eluting system $CHCl_3$/cyclohehane/EtOAc, 6:2:2). Yield, 80%; mp 192–195 °C (acetonitrile); ^{1}H NMR 7.21 (t, 1H, ar, $J = 7.3$ Hz), 7.45 (t, 2H, ar, $J = 7.9$ Hz), 7.57 (t, 2H, ar, $J = 7.5$ Hz), 7.63–7.62 (m, 2H, ar), 7.83 (d, 2H, ar, $J = 7.6$ Hz), 7.99 (d, 1H, ar, $J = 8.2$ Hz), 8.05–8.06 (m, 3H, ar), 8.54 (d, 1H, ar, $J = 8.2$ Hz), 10.96 (s, 1H, NH), 11.38 (s, 1H, NH); IR 1688; Anal. ($C_{22}H_{16}N_4O_2$) C, H, N.

General Procedure for the Synthesis of Hydrazinoquinoline-4-carboxy-(4-methoxyphenyl)amide (26) and 2-Hydrazinoquinoline-4-carboxanilide (27). A mixture of 2-chloroquinoline-4-carboxamides **24** and **25**[26,27] (3.5 mmol) and hydrazine monohydrate (4.16 mmol) in ethanol (2 mL) and water (0.5 mL) was microwave irradiated at 150 °C for 8 min. The mixture was cooled and diluted with water, and the solid was collected by filtration, washed with water, and recrystallized. **Compound 26:** yield, 75%; mp 230–231 °C (lit.[27] 229–231 °C, EtOH); ^{1}H NMR 3.73 (s, 3H, OMe), 4.48 (s, 2H, NH_2), 6.96–7.01 (m, 3H, ar), 7.23 (t, 1H, ar, $J = 7.3$ Hz), 7.54–7.64 (m, 2H, ar), 7.69 (d, 2H, ar, $J = 8.3$ Hz), 7.81 (d, 1H, ar, $J = 8.0$ Hz), 8.28 (s, 1H, NH), 10.56 (s, 1H, NHCO); Anal. ($C_{17}H_{16}N_4O_2$) C, H, N. **Compound 27:** yield, 68%; mp 226–228 °C (lit.[26] 225–227 °C, acetonitrile); ^{1}H NMR 4.42 (s, 2H, NH_2), 7.02 (s, 1H, H-3), 7.15 (t, 1H, ar, $J = 7.4$ Hz), 7.23 (t, 1H, ar, $J = 7.0$ Hz), 7.39 (t, 2H, ar, $J = 7.7$ Hz), 7.56 (t, 1H, ar, $J = 7.1$ Hz), 7.63 (d, 1H, ar, $J = 8.2$ Hz), 7.77–7.81 (m, 3H, ar), 8.23 (s, 1H, NH), 10.70 (s, 1H, NHCO); Anal. ($C_{16}H_{14}N_4O$) C, H, N.

General Procedure for the Synthesis of 2-Aminoquinoline-4-carboxy-(4-methoxyphenyl)amide (12) and 2-Aminoquinoline-4-carboxanilide (13). Compounds **26** and **27** (1.66 mmol) were dissolved in boiling EtOH (100 mL), then an excess of Ni/Raney (50% slurry in water, 4 g) was added. The suspension was hydrogenated in a Parr apparatus (50 psi) for 14 h, Ni/Raney was filtered off, and the solvent was evaporated at reduced pressure. The residue was treated with diethyl ether (4–6 mL), collected by filtration, and recrystallized. **Compound 12:** yield, 70%; mp 257–258 °C (acetonitrile); ^{1}H NMR 3.77 (s, 3H, OMe), 6.63 (s, 2H, NH_2), 6.89 (s, 1H, H-3), 6.96 (d, 2H, ar, $J = 8.96$ Hz), 7.18–7.22 (m, 1H, ar), 7.52–7.53 (m, 2H, ar), 7.69 (d, 2H, ar, $J = 8.9$ Hz), 7.78–7.80 (m, 3H, ar), 10.53 (s, 1H, NH); IR 1658, 3187, 3303, 3469; Anal. ($C_{17}H_{15}N_3O_2$) C, H, N. **Compound 13:** yield, 68%; mp 288 °C dec (2-methoxyethanol); ^{1}H NMR 6.66 (s, 2H, NH_2), 6.91 (s, 1H, H-3), 7.13–7.23 (m, 2H, ar), 7.37–7.54 (m, 4H, ar), 7.78–7.80 (m, 3H, ar), 10.69 (s, 1H, NH); IR 1628, 1662, 3192, 3298, 3467. Anal. ($C_{16}H_{13}N_3O$) C, H, N.

General Procedure for the Synthesis of 1,2-Dihydro-2-oxoquinoline-4-carboxy-(4-methoxyphenyl)amide (14) and 1,2-Dihydro-2-oxoquinoline-4-carboxyanilide (15). 2-Oxo-1,2-dihydroquinoline-4-carboxylic acid[28] (2.6 mmol) was refluxed in thionyl chloride (10 mL) for 2 h. Excess of thionyl chloride was removed at reduced pressure, and anhydrous cyclohexane (10 mL) was added to the residue and then evaporated at reduced pressure. The residue, that is, 2-oxo-quinoline-4-carbonyl chloride (**28**), was dissolved in anhydrous methylene chloride (10 mL), and the suitable aniline derivative (2.17 mmol) and triethylamine (2.17 mmol) were added to the solution. The mixture was refluxed for 1–3 h and, after cooling at room temperature, the solid was collected by filtration, washed with diethyl ether, and recrystallized. **Compound 14:** yield, 90%; mp > 300 °C (2-methoxyethanol); ^{1}H NMR 3.76 (s, 3H, OMe), 6.69 (s, 1H, H-3), 6.96 (d, 2H, ar, $J = 8.9$ Hz), 7.22 (t, 1H, ar, $J = 7.6$ Hz), 7.39 (d, 1H, ar, $J = 8.2$ Hz), 7.57 (t, 1H, ar, $J = 7.6$ Hz), 7.67 (d, 2H, ar, $J = 8.9$ Hz), 7.74 (d, 1H, ar, $J = 8.0$ Hz), 10.59 (s, 1H, NH), 11.99 (s, 1H, NH); IR 1649, 1667, 3271; Anal. ($C_{17}H_{14}N_2O_3$) C, H, N. **Compound 15:** yield, 87%; mp > 300 °C (2-methoxyethanol); ^{1}H NMR 6.71 (s, 1H, H-3), 7.16 (t, 1H, ar, $J = 7.3$ Hz), 7.23 (t, 1H, ar, $J = 7.6$), 7.37–7.39 (m, 3H, ar), 7.58 (t, 1H, ar, $J = 7.7$ Hz), 7.72–7.78 (m, 3H, ar), 10.74 (s, 1H, NH), 12.01 (s, 1H, NH); IR 1650, 1669, 3276; Anal. ($C_{16}H_{12}N_2O_2$) C, H, N.

Synthesis of the 2-Aminopyrimidine-4-carboxy-(4-methoxyphenyl)amide (16). 2-Aminopyrimidine-4-carboxylic acid[29] (5.64 mmol), 4-methoxyaniline (1.88 mmol), 1-(3-(dimethylamino)propyl))-3-ethyl-carbodiimide hydrochloride (5.64 mmol), 1-hydroxybenzotriazole (2.64 mmol), triethylamine (9.4 mmol), and 4-(dimethylamino)pyridine (0.12 mmol) in anhydrous dimethylformamide (3–4 mL) were stirred at room temperature for 44 h. The mixture was diluted with water and cooled at 0 °C. The solid, which precipitated, was collected by filtration and recrystallized. Yield, 50%; mp 215–216 °C (EtOH); ^{1}H NMR 3.75 (s, 3H, OMe), 6.94–6.97 (m, 4H, 2ar + NH_2), 7.14 (d, 1H, H-5, $J = 4.9$ Hz), 7.71 (d, 2H, ar, $J = 6.9$ Hz), 8.51 (d, 1H, ar, $J = 4.9$ Hz), 10.14 (s, 1H, NH); IR 1655, 3190, 3334; Anal. ($C_{12}H_{12}N_4O_2$) C, H, N.

Synthesis of the 2-Benzoylaminopyrimidine-4-carboxy-(4-methoxyphenyl)amide (17) and 2-Dibenzoylaminopyrimidine-4-carboxy-(4-methoxyphenyl)amide (18). A mixture of compound **16** (1.31 mmol), benzoyl chloride (2.32 mmol), and anhydrous pyridine (4.96 mmol) in anhydrous methylene chloride (20 mL) was refluxed for 48 h. The solid was filtered off and the methylene chloride solution was washed with water (2 × 10 mL). The anhydrified (Na_2SO_4) organic phase was evaporated at reduced pressure. The solid residue was a mixture of compounds **17** and **18**, which were separated by column chromatography (SiO_2, eluting system EtOAc/CH_2Cl_2, 1:9). **Compound 17:** yield, 15%; mp 197–199 °C (EtOH); ^{1}H NMR 3.76 (s, 3H, OMe), 6.99 (d, 2H, ar, $J = 9.0$ Hz), 7.57 (t, 2H, ar, $J = 7.8$ Hz), 7.64 (t, 1H, ar, $J = 7.8$ Hz), 7.71 (d, 2H, ar, $J = 9.0$ Hz), 7.80 (d, 1H, H-5, $J = 4.9$ Hz), 8.01 (d, 2H, ar, $J = 7.5$ Hz), 9.02 (d, 1H, H-6, $J = 4.9$ Hz), 10.26 (s, 1H, NH), 11.23 (s, 1H, NH); IR 1660, 1681, 3225, 3305; Anal. ($C_{19}H_{16}N_4O_3$) C, H, N. **Compound 18:** yield, 45%; mp 230–232 °C (EtOH); ^{1}H NMR 3.75 (s, 3H, OMe), 6.95 (d, 2H, ar, J= 9.1 Hz), 7.47–7.65 (m, 8H, ar), 7.84 (d, 4H, ar, $J = 7.7$ Hz), 7.91 (d, 1H, H-5), 9.01 (d, 1H, H-6, $J = 5.0$ Hz), 10.09 (s, 1H, NH); IR 1681, 1695, 3351; Anal. ($C_{26}H_{20}N_4O_4$) C, H, N.

(C) Pharmacological Assays. Human Cloned A_1, A_{2A}, and A_3 Adenosine Receptor Binding Assay. All synthesized compounds were tested for evaluating their affinity at human A_1, A_{2A}, and A_3 adenosine receptors. Displacement experiments of [^{3}H]-DPCPX (1 nM) to hA_1 CHO membranes (50 μg of protein/assay) and at least 6–8 different concentrations of antagonists for 120 min at 25 °C in 50 mM Tris HCl buffer, pH 7.4, were performed.[30] Nonspecific binding was determined in the presence of 10 μM of CHA (≤10% of the total binding). Binding of [^{3}H]ZM-241385 (1 nM) to hA_{2A} CHO membranes (50 μg of protein/assay) was performed by using 50 mM Tris HCl buffer, 10 mM $MgCl_2$, pH 7.4, and at least 6–8 different concentrations of antagonists studied for an incubation time of 60 min at 4 °C.[31] Nonspecific binding was determined in the presence of 1 μM ZM-241385 and was about 20% of total binding. Competition binding experiments to hA_3 CHO

membranes (50 μg of protein/assay) and 0.5 nM [^{125}I]AB-MECA, 50 mM Tris HCl buffer, 10 mM $MgCl_2$, 1 mM EDTA, pH 7.4, and at least 6–8 different concentrations of examined ligands for 120 min at 4 °C.[32] Nonspecific binding was defined as binding in the presence of 1 μM AB-MECA and was about 20% of total binding. Bound and free radioactivity were separated by filtering the assay mixture through Whatman GF/B glass fiber filters by using a Brandel cell harvester. The filter bound radioactivity was counted by Scintillation Counter Packard Tri Carb 2500 TR with an efficiency of 58%.

Measurement of Cyclic AMP Levels in CHO Cells Transfected with hA_{2B} or hA_3 Adenosine Receptors. CHO cells transfected with hAR subtypes were washed with phosphate-buffered saline and diluted tripsine and centrifuged for 10 min at 200 *g*. The pellet containing the CHO cells (1×10^6 cells /assay) was suspended in 0.5 mL of incubation mixture (mM): NaCl, 15; KCl, 0.27; NaH_2PO_4, 0.037; $MgSO_4$, 0.1; $CaCl_2$, 0.1; Hepes, 0.01; $MgCl_2$, 1; glucose, 0.5; pH 7.4, at 37 °C, 2 IU/ml adenosine deaminase and 4-(3-butoxy-4-methoxybenzyl)-2-imidazolidinone (Ro 20–1724) as phosphodiesterase inhibitor and preincubated for 10 min in a shaking bath at 37 °C. The potency of antagonists to A_{2B} receptors was determined by antagonism of NECA (200 nM)-induced stimulation of cyclic AMP levels. In addition, the potency of antagonists to A_3 receptors was determined in the presence of forskolin 1 μM and Cl-IB-MECA (100 nM) that mediated inhibition of cyclic AMP levels. The reaction was terminated by the addition of cold 6% trichloroacetic acid (TCA). The TCA suspension was centrifuged at 2000 *g* for 10 min at 4 °C, and the supernatant was extracted four times with water-saturated diethyl ether. The final aqueous solution was tested for cyclic AMP levels by a competition protein binding assay. Samples of cyclic AMP standard (0–10 pmoles) were added to each test tube containing [^{3}H] cyclic AMP and the incubation buffer (trizma base, 0.1 M; aminophylline, 8.0 mM; 2-mercaptoethanol, 6.0 mM; pH 7.4). The binding protein prepared from beef adrenals, was added to the samples previously incubated at 4 °C for 150 min and, after the addition of charcoal, were centrifuged at 2000 *g* for 10 min. The clear supernatant was counted in a Scintillation Counter Packard Tri Carb 2500 TR with an efficiency of 58%.[33]

Data Analysis

The protein concentration was determined according to a Bio-Rad method,[34] with bovine albumin as a standard reference. Inhibitory binding constant, K_i, values were calculated from those of IC_{50} according to Cheng−Prusoff equation: $K_i = IC_{50}/(1 + [C^*]/K_D^*)$, where $[C^*]$ is the concentration of the radioligand and K_D^* is the dissociation constant.[35] A weighted nonlinear least-squares curve fitting program LIGAND[36] was used for computer analysis of inhibition experiments. EC_{50} and IC_{50} values obtained in the cyclic AMP assay were calculated by nonlinear regression analysis using the equation for a sigmoid concentration–response curve (Graph-PAD Prism, San Diego, CA, U.S.A).

Acknowledgment. The molecular modeling work coordinated by S.M. has been carried out with financial support from the University of Padova, Italy, and the Italian Ministry for University and Research (MIUR), Rome, Italy. S.M. is also very grateful to Chemical Computing Group for the scientific and technical partnership. The synthetic work was supported by a grant of the Italian Ministry for University and Research (MIUR, FIRB RBNE03YA3L project).

Supporting Information Available: Combustion analysis data of the synthesized compounds. This material is available free of charge via the Internet at http://pubs.acs.org.

References

(1) Jacobson, K. A.; Knutsen, L. J. S. P1 and P2 purine and pyrimidine receptor ligands. In *Purinergic and Pyrimidinergic Signalling (Handbook of Experimental Pharmacology)*; Abbracchio, M. P., Williams, M., Eds; Springer: Berlin, 2001; Vol. *151/1*, pp 129–175.
(2) Jacobson, K. A.; Gao, Z. G. Adenosine receptors as therapeutic targets. *Nat. Rev. Drug Discovery* **2006**, *5*, 247–264.
(3) Schulte, G.; Fredholm, B. B. Signaling from adenosine receptors to mitogen-activated protein kinases. *Cell. Signal.* **2003**, *15*, 813–827.
(4) Wymann, M. P.; Bjorklof, K.; Calvez, R.; Finan, P.; Thomast, M.; Trifilieff, A. Phosphoinositide 3-kinase γ: a key modulator in inflammation and allergy. *Biochem. Soc. Trans.* **2003**, *31*, 275–280.
(5) Hammarberg, C.; Fredholm, B. B.; Schulte, G. Adenosine A_3 receptor-mediated regulation of p38 and extracellular-regulated kinase ERK1/2 via phosphatidylinositol-3′-kinase. *Biochem. Pharmacol.* **2004**, *67*, 129–134.
(6) Laffargue, M.; Calvez, R.; Finan, P.; Trifilieff, A.; Barbier, M.; Altruda, F. Phosphoinositide 3-kinase γ is an essential amplifier of mast cell function. *Immunity* **2002**, *16*, 441–451.
(7) Trincavelli, M. L.; Tuscano, D.; Marroni, M.; Klotz, K. N.; Lucacchini, A.; Martini, C. Involvement of mitogen protein kinase cascade in agonist-mediated human A_3 adenosine receptor regulation. *Biochim. Biophys. Acta* **2002**, *1591*, 55–62.
(8) Rorke, S.; Holgate, S. T. Targeting adenosine receptors: Novel therapeutic targets in asthma and chronic obstructive pulmonary disease. *Am. J. Respir. Med.* **2002**, *1*, 99–105.
(9) Jacobson, K. A. Adenosine A_3 receptors: novel ligands and paradoxical effects. *Trends Pharmacol. Sci.* **1998**, *19*, 184–191.
(10) Stone, T. W. Purines and neuroprotection. *Adv. Exp. Med. Biol.* **2002**, *513*, 249–280.
(11) Moro, S.; Gao, Z. G.; Jacobson, K. A.; Spalluto, G. Progress in the pursuit of therapeutic adenosine receptor antagonists. *Med. Res. Rev.* **2006**, *26*, 131–159.
(12) Moro, S.; Deflorian, F.; Spalluto, G.; Pastorin, G.; Cacciari, B.; et al. Demystifying the three dimensional structure of G-protein-coupled receptors (GPCRs) with the aid of molecular modeling. *Chem. Commun. (Cambridge)* **2003**, *24*, 2949–2956.
(13) Moro, S.; Spalluto, G.; Jacobson, K. A. Techniques: Recent developments in computer-aided engineering of GPCR ligands using the human A_3 adenosine receptor as an example. *Trends Pharmacol. Sci.* **2005**, *26*, 44–51.
(14) Moro, S.; Braiuca, P.; Deflorian, F.; Ferrari, C.; Pastorin, G.; Cacciari, B.; Baraldi, P. G.; Varani, K.; Borea, P. A.; Spalluto, G. Combined target-based and ligand-based drug design approach as tool to define a novel 3D-pharmacophore model of human A_3 adenosine receptor antagonists: Pyrazolo[4,3-*e*]1,2,4-triazolo[1,5-*c*]pyrimidine derivatives as a key study. *J. Med. Chem.* **2005**, *48*, 152–162.
(15) Moro, S.; Bacilieri, M.; Cacciari, B.; Spalluto, G. Autocorrelation of molecular electrostatic potential surface properties combined with partial least squares analysis as new strategy for the prediction of the activity of human A_3 adenosine receptor antagonists. *J. Med. Chem.* **2005**, *48*, 5698–5704.
(16) Moro, S.; Bacilieri, M.; Deflorian, F.; Spalluto, G. G-protein-coupled receptors as challenging druggable targets: insights from in silico studies. *New J. Chem.* **2006**, *30*, 301–308.
(17) Moro, S.; Deflorian, F.; Bacilieri, M.; Spalluto, G. Novel strategies for the design of new potent and selective human A_3 receptor antagonists: an update. *Curr. Med. Chem.* **2006**, *13*, 639–645.
(18) Colotta, V.; Catarzi, D.; Varano, F.; Cecchi, L.; Filacchioni, G.; Martini, C.; Trincavelli, L.; Lucacchini, A. 1,2,4-Triazolo[4,3-*a*]quinoxalin-1-one: A versatile tool for the synthesis of potent and selective adenosine receptor antagonists. *J. Med. Chem.* **2000**, *43*, 1158–1164.
(19) Colotta, V.; Catarzi, D.; Varano, F.; Filacchioni, G.; Martini, C.; Trincavelli, L.; Lucacchini, A. Synthesis and structure−activity relationships of a new set of 1,2,4-triazolo[4,3-*a*]quinoxalin-1-one derivatives as adenosine receptor antagonists. *Bioorg. Med. Chem.* **2003**, *11*, 3541–3550.
(20) Colotta, V.; Catarzi, D.; Varano, F.; Filacchioni, G.; Martini, C.; Trincavelli, L.; Lucacchini, A. Synthesis of 4-amino-6-(hetero)arylalkylamino-1,2,4-triazolo[4,3-*a*]quinoxalin-1-one derivatives as potent A_{2A} adenosine receptor antagonists. *Bioorg. Med. Chem.* **2003**, *11*, 5509–5518.
(21) Colotta, V.; Catarzi, D.; Varano, F.; Calabri, F. R.; Lenzi, O.; Filacchioni, G.; Trincavelli, L.; Martini, C.; Deflorian, F.; Moro, S. 1,2,4-Triazolo[4,3-*a*]quinoxalin-1-one moiety as an attractive scaffold to develop new potent and selective human A_3 adenosine receptor antagonists: Synthesis, pharmacological, and ligand−receptor modeling studies. *J. Med. Chem.* **2004**, *47*, 3580–3590.
(22) Catarzi, D.; Colotta, V.; Varano, F.; Calabri, F. R.; Lenzi, O.; Filacchioni, G.; Trincavelli, L.; Martini, C.; Tralli, A.; Montopoli, C.; Moro, S. 2-Aryl-8-chloro-1,2,4-triazolo[1,5-*a*]quinoxalin-4-amines as highly potent A_1 and A_3 adenosine receptor antagonists. *Bioorg. Med. Chem.* **2005**, *13*, 705–715.
(23) Catarzi, D.; Colotta, V.; Varano, F.; Lenzi, O.; Filacchioni, G.; Trincavelli, L.; Martini, C.; Montopoli, C.; Moro, S. 1,2,4-Triazolo[1,5-*a*]quinoxaline as a versatile tool for the design of selective human A_3

adenosine receptor antagonists: Synthesis, biological evaluation, and molecular modeling studies of 2-(hetero)aryl- and 2-carboxy-substituted derivatives. *J. Med. Chem.* **2005**, *48*, 7932–7945.

(24) Lenzi, O.; Colotta, V.; Catarzi, D.; Varano, F.; Filacchioni, G.; Martini, C.; Trincavelli, L.; Ciampi, O.; Marighetti, F.; Morizzo, E.; Moro, S. 4-Amido-2-aryl-1,2,4-triazolo[4,3-*a*]quinoxalin-1-ones as new potent and selective human A_3 adenosine receptor antagonists. Synthesis, pharmacological evaluation, and ligand−receptor modeling studies. *J. Med. Chem.* **2006**, *49*, 3916–3925.

(25) Stefanovich, G. J.; Lorenc, L. J.; Mihailovic, M. L. J. Condensations of isatinic acid with ureas, ethyl carbamate, and guanidine. *Rec. Trav. Chim.* **1961**, *80*, 149–157.

(26) Yanborisova, O. Y.; Kon'shin, M. E. Synthesis of substituted 2-hydrazino- and 2-(β-acylhydrazino)-cinchoninic acid amides and their cyclization to 1,2,4-triazolo[4,3-*a*]quinoline-9-carboxylic acid amides. *Chem. Heterocycl. Compd. (N.Y.)* **1991**, *27*, 390–394.

(27) Yanborisova, O. Y.; Kon'shina, T. M.; Zaks, a. S.; Mikhalev, A. I.; Kon'shin, M. E. Synthesis and biological activity of amides of hydrazinocinchoninic, 1,2,4-triazolo[4,3-*a*]-, and 1,2,3,4-tetrazolo[4,3-*a*]-quinoline-9-carboxylic acids. *Pharm. Chem. J.* **1996**, *30*, 197–199.

(28) El Ashry, E. S. H.; Ramadan, E. S.; Hamid, H. A.; Hagar, M. Microwave-assisted synthesis of quinoline derivatives from isatin. *Synth. Commun.* **2005**, *35*, 2243–2250.

(29) Daves, G. D., Jr; O'Brien, D. E.; Lewis, L. R.; Cheng, C. C. Pyrimidines. XIII. 2-Substituted and 6-substituted 4-pyrimidinecarboxylic acids. *J. Heterocycl. Chem.* **1964**, *1*, 130–133.

(30) Borea, P. A.; Dalpiaz, A.; Varani, K.; Gessi, S.; Gilli, G. Binding thermodynamics at A_1 and A_{2A} adenosine receptors. *Life Sci.* **1996**, *59*, 1373–88.

(31) Varani, K.; Rigamonti, D.; Sipione, S.; Camurri, A.; Borea, P. A.; Cattabeni, F.; Abbracchio, M. P.; Cattaneo, E. Aberrant amplification of A_{2A} receptor signalling in striatal cells expressing mutant huntigtin. *FASEB J.* **2001**, *5*, 1245–1247.

(32) Varani, K.; Cacciari, B.; Baraldi, P. G.; Dionisotti, S.; Ongini, E.; Borea, P. A. Binding affinity of adenosine receptor agonists and antagonists at human cloned A_3 adenosine receptors. *Life Sci.* **1998**, *63*, 81–87.

(33) Varani, K.; Gessi, S.; Merighi, S.; Vincenzi, F.; Cattabriga, E.; Benini, A.; Klotz, K.-N.; Baraldi, P. G.; Tabrizi, M.-A.; Mac Lennan, S.; Leung, E.; Borea, P. A. Pharmacological characterization of novel adenosine ligands in recombinant and native human A_{2B} receptors. *Biochem. Pharmacol.* **2005**, *70*, 1601–1612.

(34) Bradford, M. M. A rapid and sensitive method for the quantification of microgram quantities of protein utilizing the principle of protein dye-binding. *Anal. Biochem.* **1976**, *72*, 248–254.

(35) Cheng, Y. C.; Prusoff, W. H. Relationships between the inhibition constant (K_i) and the concentration of inhibitor which causes 50% inhibition (IC_{50}) of an enzymatic reaction. *Biochem. Pharmacol.* **1973**, *22*, 3099–3108.

(36) Munson, P. J.; Rodbard, D. Ligand: a versatile computerized approach for the characterization of ligand binding systems. *Anal. Biochem.* **1980**, *107*, 220–239.

(37) *Molecular Operating Environment*,version 2006.08; Chemical Computing Group: Montreal, Canada, 2006.

(38) *MOPAC* ,version 7; Stewart, J. J. P., Ed.; Fujitsu Limited: Tokyo, Japan, 1993.

(39) Palczewski, K.; Kumasaka, T.; Hori, T.; Behnke, C. A.; Motoshima, H. Crystal structure of rhodopsin: A G-protein-coupled receptor. *Science* **2000**, *289*, 739–745.

(40) Cornell, W. D. C., P.; Bayly, C. I.; Gould, I. R.; Merz, K. M.; Ferguson, D. M.; Spellmeyer, D. C.; Fox, T.; Caldwell, J. W.; Kollman, P. A. A second generation force field for the simulation of proteins, nucleic acids and organic molecules. *J. Am. Chem. Soc.* **1995**, *117*, 5179–5196.

(41) Moro, S.; Deflorian, F.; Bacilieri, M.; Spalluto, G. Ligand-based homology modeling as attractive tool to inspect GPCR structural plasticity. *Curr. Pharm. Des.* **2006**, *12*, 2175–2185.

(42) Baxter, C. A.; Murray, C. W.; Clark, D. E.; Westhead, D. R.; Eldridge, M. D. Flexible Docking Using Tabù Search and an Empirical Estimate of Binding Affinity. *Proteins: Struct., Funct., Genet.* **1998**, *33*, 367–382.

(43) Halgren, T. Merck molecular force field. I. Basis, form, scope, parameterization, and performance of MMFF94. *J. Comput. Chem.* **1996**, *17*, 490–519.

JM070852A